



POLITECNICO DI TORINO  
Repository ISTITUZIONALE

Modeling Orbital Angular Momentum (OAM) Transmission in Waveguides with the COMSOL Multiphysics® Software

*Original*

Modeling Orbital Angular Momentum (OAM) Transmission in Waveguides with the COMSOL Multiphysics® Software / Cagliero, Andrea; De Vita, Assunta; Gaffoglio, Rossella; Sacco, Bruno. - ELETTRONICO. - (2016). ((Intervento presentato al convegno COMSOL Conference 2016 tenutosi a Munich nel 12-14 October 2016.

*Availability:*

This version is available at: 11583/2731420 since: 2019-04-23T18:35:29Z

*Publisher:*

COMSOL Multiphysics

*Published*

DOI:

*Terms of use:*

openAccess

This article is made available under terms and conditions as specified in the corresponding bibliographic description in the repository

*Publisher copyright*

(Article begins on next page)

# Modeling OAM Transmission in Waveguides with COMSOL Multiphysics

A. Cagliero<sup>1\*</sup>, A. De Vita<sup>2</sup>, R. Gaffoglio<sup>1</sup> and B. Sacco<sup>2</sup>

<sup>1</sup> Department of Physics, University of Torino, Torino, Italy

<sup>2</sup> Centre for Research and Technological Innovation, RAI Radiotelevisione Italiana, Torino, Italy

\* Corresponding author: andrea.cagliero@unito.it

**Abstract:** The recent years have witnessed a growing interest in the possibility of enhancing the information transfer per unit bandwidth by exploiting the Orbital Angular Momentum (OAM) of light in both free-space and guided scenarios. In the proposed paper, the propagation of suitable OAM superpositions of waveguide eigenmodes in guiding structures with a circular symmetry is analyzed both theoretically and with the aid of the software COMSOL Multiphysics®, leading to the estimation of the power attenuation constants due to the finite conductivity of the metallic guide walls.

**Keywords:** Circular waveguide; coaxial cable; COMSOL Multiphysics; Orbital Angular Momentum (OAM).

## 1. Introduction

As emphasized in literature [1], the free-space propagation of OAM beams is affected by an over-quadratic power decay with distance. However, this negative aspect does not concern guided propagation of waves carrying OAM, which is instead free from this limitation. This fact has favored the interest towards the possibility of exploiting the OAM in waveguide scenarios, where vortex beams can be thought as suitable superpositions of the standard Transverse Electric (TE) or Transverse Magnetic (TM) modes supported by the considered guiding structures [2].

In Optics, the possibility to excite OAM modes in fibers has been experimentally verified first in particular kind of fibers [3,4], with ring-shaped cores, and then in conventional optical fibers [5], paving the way to the realization of OAM-based multiplexing schemes [5,6]. The guided propagation of OAM modes has been also considered at the radio frequencies and in the microwave band, since waveguides are often part of radiating systems [7,8]; as an example, this is the case of the horn antennas, which

consist of a flared metal waveguide shaped like a horn [9].

According to the considerations reported in [2], in hollow metallic waveguides with a circular symmetry, trivial combinations of the conventional eigenmodes are able to carry angular momentum, including both an OAM and a SAM (Spin Angular Momentum) contribution. In this work, the propagation of these modes in circular waveguides and coaxial cables will be investigated both theoretically and also by means of numerical simulations performed with the RF module of the software COMSOL Multiphysics. The presented analysis will explicitly prove how such OAM superpositions can be supported by the considered guiding structures at frequencies greater than the corresponding cutoff values. Then, the power attenuation law relative to the propagation of different OAM modes inside a circular waveguide with copper walls will be presented, as a result of a realistic electromagnetic simulation.

## 2. Circular waveguide

Any perturbation inside a circular waveguide with metallic walls can be described in terms of TE and TM modes, properly obtained by solving the Maxwell's macroscopic equations with the boundary conditions dictated by the waveguide geometry. Therefore, these electromagnetic modes, whose mathematical expression is derived in [10,11], constitute a complete set of fields inside the circular waveguide.

In this section the TE modes for a circular waveguide with uniform cross section and perfectly conducting walls are explicitly reported. Then, it will be shown how to obtain propagating modes carrying OAM by superimposing pairwise such conventional eigenmodes.

By definition, a transverse electric mode has no electric field in the direction of propagation, i.e.,  $E_z = 0$ . According to [11], the transverse

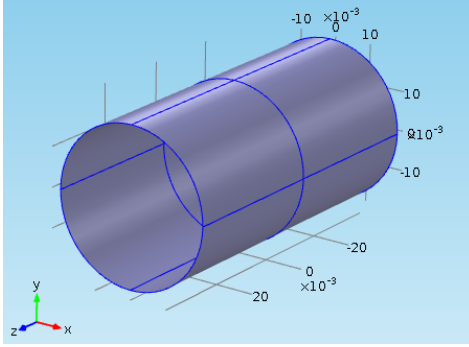


**Figure 1.** Circular waveguide oriented along the  $z$ -axis and simulated with the software COMSOL Multiphysics.

electric field components of a TE mode propagating inside a circular waveguide of radius  $a$  can be written as:

$$E_\rho = \frac{i}{\gamma_{nj}^2} k_0 c \frac{n}{\rho} B_0 J_n(\gamma_{nj} \rho) \cdot [-A \cos(n\varphi) + B \sin(n\varphi)] e^{-i\alpha_{nj} z} \quad (1)$$

$$E_\varphi = \frac{i}{\gamma_{nj}} k_0 c B_0 J'_n(\gamma_{nj} \rho) \cdot [A \sin(n\varphi) + B \cos(n\varphi)] e^{-i\alpha_{nj} z} \quad (2)$$

where the harmonic time dependence has been omitted,  $B_0$  is a constant with magnetic field dimensions,  $A$  and  $B$  are arbitrary adimensional constants, while  $\gamma_{nj} = \zeta_{nj}/a$ , being  $\zeta_{n1}, \zeta_{n2}, \dots, \zeta_{nj}$  the non-null positive zeros of the function  $J'_n(\zeta)$ , arranged by increasing magnitude. The indices  $n$  and  $j$  indicate a transverse electric mode propagating inside the waveguide with a wavenumber  $\alpha_{nj}$  given by:

$$\alpha_{nj} = \sqrt{\varepsilon_r \mu_r k_0^2 - \gamma_{nj}^2}, \quad (3)$$

being  $\varepsilon_r$  and  $\mu_r$  the relative permittivity and permeability of the interior medium. It should be noted that such mode can exist inside the waveguide if and only if the operating frequency  $\omega$  is greater than the corresponding cutoff frequency  $\gamma_{nj}/\sqrt{\varepsilon\mu}$ , where  $\varepsilon$  and  $\mu$  are the absolute permittivity and permeability. Since the lowest zero of the first derivative of the Bessel function  $J_n$  is  $\zeta_{11}$ , it follows that the TE mode which can propagate inside the waveguide at the lowest frequency is the TE<sub>11</sub>.

The two sets of modes TE<sub>cnj</sub>, with  $A \neq 0$  and  $B = 0$ , and TE<sub>snj</sub>, with  $A = 0$  and  $B \neq 0$ , completely span the orthogonal set of transverse electric modes inside the waveguide. By redefining these modes in such a way that the parameters  $A$  and  $B$  fulfill  $A = iB$  or  $A = -iB$ , the following new complete set of orthogonal modes can be obtained [2]:

$$\text{TE}_{cnj} \pm i \text{TE}_{snj}. \quad (4)$$

Using the expressions for the TE modes reported in (1) and (2), the electric field components relative to the superpositions defined in (4) can be explicitly written as:

$$E_\rho = -\frac{i}{\gamma_{nj}^2} k_0 c \frac{n}{\rho} B_0 K_\pm J_n(\gamma_{nj} \rho) e^{\mp in\varphi} e^{-i\alpha_{nj} z} \quad (5)$$

$$E_\varphi = \mp \frac{1}{\gamma_{nj}} k_0 c B_0 K_\pm J'_n(\gamma_{nj} \rho) e^{\mp in\varphi} e^{-i\alpha_{nj} z} \quad (6)$$

where  $K_\pm$  is a new adimensional constant.

In [2] it has been demonstrated that the modes defined in (5),(6) carry a net angular momentum which is, on average,  $\pm n\hbar$  per photon. This quantity includes both an OAM and a SAM (Spin Angular Momentum) contribution. It is indeed impossible for an electromagnetic mode to propagate inside the waveguide carrying all its angular momentum either in the form of spin or OAM. The combinations defined in (4) represent nothing but a particular basis choice in the space of the waveguide eigenmodes and the mode density of the two sets is the same [2].

In order to visualize these modes and to prove their propagation in a circular waveguide, the analytic expression of the electric field (5),(6) is provided in input to a circular waveguide modeled with the RF module of the software COMSOL Multiphysics (see Fig. 1). The radius of the circular waveguide is assumed to be  $a = 0.02$  m, the interior region is filled with air and a Perfect Electric Conductor (PEC) condition is imposed on the walls. Fig. 2 and 3 show the intensity profiles of two superpositions like (4), with  $j = 1$  and  $n = 0, 1$ , at an operating frequency  $f = 10$  GHz, sufficient to allow the propagation of these modes inside the considered waveguide.

It is worth noting that the above presented approach could be extended to the TM modes, for which superpositions carrying angular momentum are defined in complete analogy to (4).

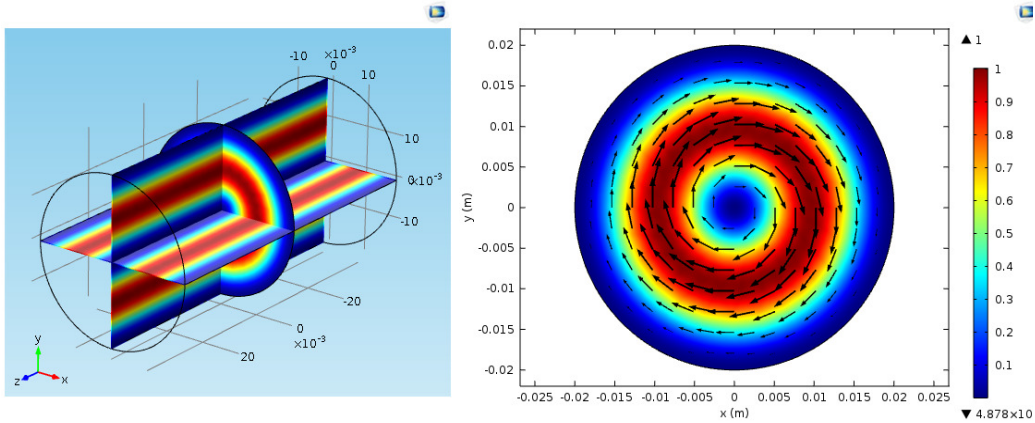


**Figure 2.** Normalized electric field intensity for the superposition  $TE_{c01} - iTE_{s01}$  evaluated with the software COMSOL Multiphysics in a circular waveguide of radius  $a = 0.02$  m. The real part of the vector field over the middle transverse cross section is also reported.

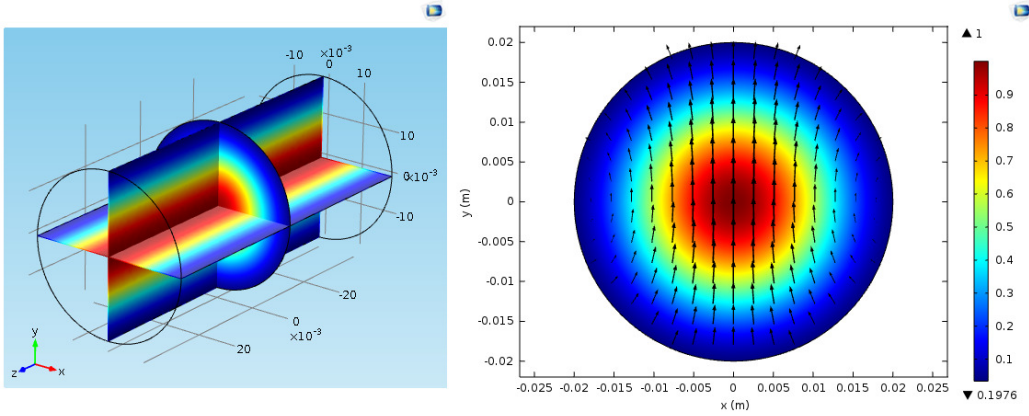


**Figure 3.** Normalized electric field intensity for the superposition  $TE_{c11} - iTE_{s11}$  evaluated with the software COMSOL Multiphysics in a circular waveguide of radius  $a = 0.02$  m.

### 3. Coaxial cable

A coaxial cable is made by an inner conducting wire sequentially surrounded by a tubular insulating layer and an external metallic shield. This kind of structure can be viewed as a type of waveguide able to support the propagation of the Transverse Electric and Magnetic (TEM) mode (neither electric nor magnetic field in the direction of propagation), by virtue of the presence of two conductors. When it exists, like in a coaxial cable, the TEM mode is the fundamental one, having no cutoff frequency. Despite this, in order to obtain modes able to carry angular momentum, it is necessary to resort to the higher-

order TE (or TM) modes, whose formulation for the coaxial cable will be introduced in the following.

According to the approach presented in [11], the electric field components of a TE mode propagating inside a coaxial cable with outer radius  $a$  and inner radius  $b$  can be written as:

$$E_{\rho} = \frac{i}{\chi_{nj}^2} k_0 c \frac{n}{\rho} B_0 [Y'_n(\chi_{nj} a) J_n(\chi_{nj} \rho) - J'_n(\chi_{nj} a) \cdot Y_n(\chi_{nj} \rho)] [-A \cos(n\varphi) + B \sin(n\varphi)] e^{-i\alpha_{nj} z} \quad (7)$$

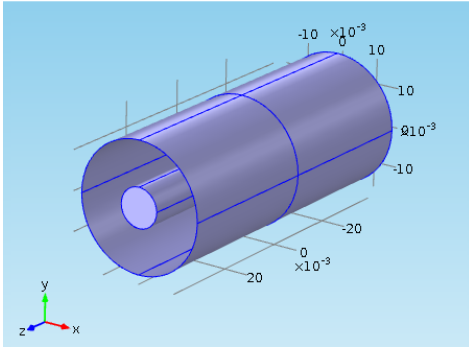


**Figure 4.** Coaxial cable oriented along the  $z$ -axis and simulated with the software COMSOL Multiphysics.

$$E_\varphi = \frac{i}{\chi_{nj}} k_0 c B_0 [Y'_n(\chi_{nj} a) J'_n(\chi_{nj} \rho) - J'_n(\chi_{nj} a) \cdot Y'_n(\chi_{nj} \rho)] [A \sin(n\varphi) + B \cos(n\varphi)] e^{-i\alpha_{nj} z} \quad (8)$$

where  $B_0$  is a constant with the dimensions of a magnetic field,  $A$ ,  $B$  and  $K$  are adimensional constants, while  $\chi_{n1}, \chi_{n2}, \dots, \chi_{nj}$  are the solutions, sorted by increasing magnitude, of the following transcendental equation:

$$J'_n(\chi a) Y'_n(\chi b) - J'_n(\chi b) Y'_n(\chi a) = 0. \quad (9)$$

A frequency  $\omega$  greater than the cutoff value  $\chi_{nj} / \sqrt{\epsilon \mu}$  allows the propagation of the  $TE_{nj}$  mode inside the coaxial cable, with a wavenumber:

$$\alpha_{nj} = \sqrt{\epsilon_r \mu_r k_0^2 - \chi_{nj}^2}. \quad (10)$$

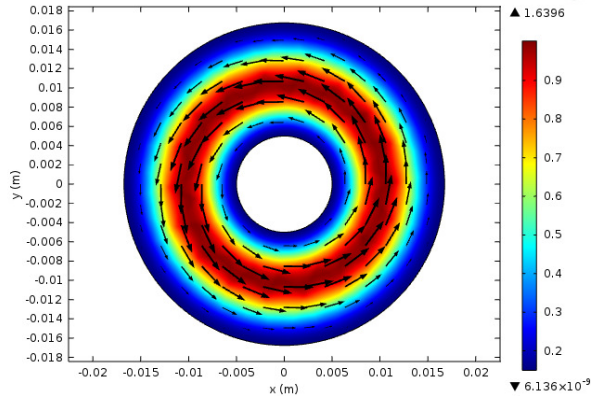
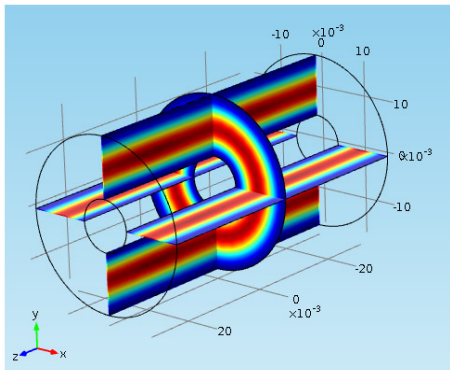


**Figure 5.** Normalized electric field intensity for the  $n = 0$  TE superposition evaluated with the software COMSOL Multiphysics in a coaxial cable filled with Teflon. The real part of the vector field over the middle transverse cross section is also reported.

Following the same approach presented in the previous section for the circular waveguide, the TE components (7), (8), relative to the coaxial cable, can be superimposed pairwise according to the combination defined in (4), leading to:

$$E_\rho = -\frac{i}{\chi_{nj}^2} k_0 c \frac{n}{\rho} B_0 K_\pm [Y'_n(\chi_{nj} a) J_n(\chi_{nj} \rho) + J'_n(\chi_{nj} a) Y_n(\chi_{nj} \rho)] e^{\mp in\varphi} e^{-i\alpha_{nj} z} \quad (11)$$

$$E_\varphi = \mp \frac{1}{\chi_{nj}} k_0 c B_0 K_\pm [Y'_n(\chi_{nj} a) J'_n(\chi_{nj} \rho) + J'_n(\chi_{nj} a) Y'_n(\chi_{nj} \rho)] e^{\mp in\varphi} e^{-i\alpha_{nj} z} \quad (12)$$

The propagation of these modes can be verified with the aid of the software COMSOL Multiphysics by properly feeding the input port of a coaxial cable (Fig. 4) with the considered superpositions of TE modes. The inner and outer conductors of the simulated coaxial cable are modeled with a Perfect Electric Conductor condition imposed on their surfaces, while the inner region is filled with a Teflon dielectric layer ( $\epsilon_r = 2.1$ ,  $\mu_r = 1$ ). Moreover, the radii of the two conductors are assumed to be:  $a = 0.016$  m and  $b = 0.005$  m.

Fig. 5 and 6 show the electric field intensity for the combinations  $TE_{cnj} - iTE_{snj}$ , with  $j = 1$  and  $n = 0, 1$ , propagating inside the considered coaxial cable at an operating frequency  $f = 10$  GHz.

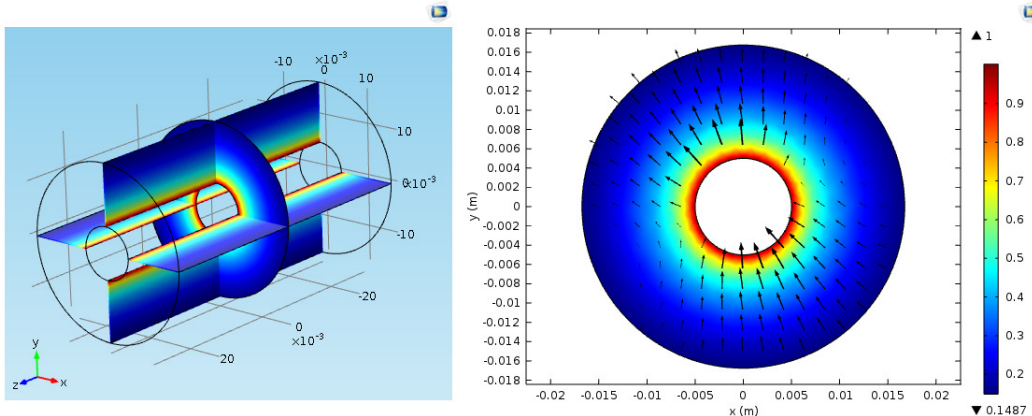


**Figure 6.** Normalized electric field intensity for the  $n = 1$  TE superposition evaluated with the software COMSOL Multiphysics in a coaxial cable filled with Teflon.

#### 4. Power attenuation law

The waveguides considered so far have been ideally supposed to be made of perfect conductors. Inside this kind of waveguides the electromagnetic modes can propagate above the cutoff without suffering any attenuation. However, in practice, perfect conductors do not exist, but rather there are good conducting materials, such as metals, with finite conductivities on the order of  $10^7$ - $10^8$  S/m. These great, but limited, values of the metal conductivity causes the field to penetrate a little the waveguide walls; as a consequence, the conduction electrons of the metal layer are set into motion, dissipating a part of the energy via the Joule effect. Hence, in real waveguides with metallic walls, the supported electromagnetic modes undergo some attenuation due to the conduction (ohmic) losses. Moreover, if the considered waveguide is filled with a lossy dielectric material, the so-called dielectric losses introduce a further contribution to the waveguide attenuation. Anyway, restricting the present analysis to the case of waveguides filled with air, such kind of losses can be neglected.

If  $P_0$  represents the power associated to a mode with indices  $(n, j)$  at some reference point along the guiding direction (i.e.,  $z = 0$ ), then the power  $P$  at some other point  $z$  is related to  $P_0$  by:

$$P(z) = P_0 e^{-2\beta_{nj}z}, \quad (13)$$

where  $\beta_{nj}$  is the ohmic losses attenuation coefficient.

In order to estimate the attenuation coefficient relative to the propagation of a superposition  $TE_{cnj} \pm iTE_{snj}$  inside a real guiding structure, a circular waveguide with copper walls is simulated with the software COMSOL Multiphysics. The modeled waveguide is filled with air, the radius is assumed to be  $a = 0.02$  m and the operating frequency  $f$  is fixed at 10 GHz. By means of a parametric sweep, COMSOL provides the estimation of the  $S_{21} = P(z)/P_0$  parameter for different values of the waveguide length  $z$ , between  $2\lambda$  and  $102\lambda$ , being  $\lambda$  the wavelength. Fig. 7 shows the  $S_{21}$  parameters as a function of  $z$  in logarithmic scale, for three different TE mode superpositions with indices  $j = 1$  and  $n = 0, 1, 2$ . For each of the considered cases a linear fit is performed enabling the estimation of the corresponding power attenuation constants.

The same procedure is then repeated for the propagation of single  $TE_{nj}$  modes, with  $j = 1$  and  $n = 0, 1, 2$ . As can be seen from Table 1, the attenuation coefficients estimated for the TE modes coincide with those obtained for the OAM superpositions. As expected, this result shows that the waveguide mode combinations able to carry angular momentum exhibit the same behaviour in terms of power budget as the conventional modes.

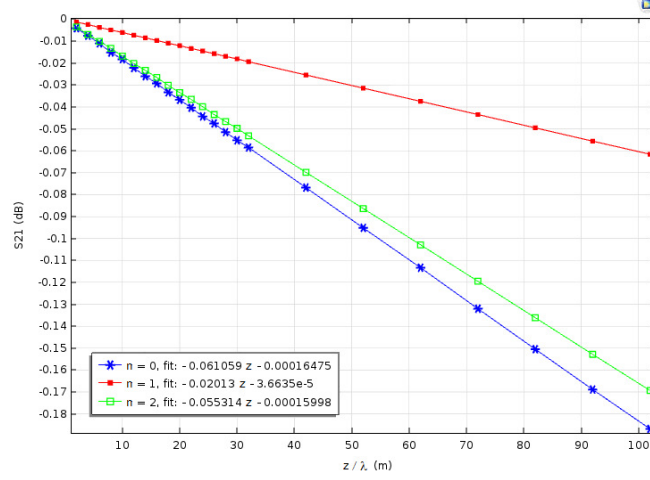


**Figure 7.**  $S_{21}$  parameter as a function of the guide length  $z$  for a circular waveguide with copper walls and radius  $a = 0.02$  m. In the legend the results of the corresponding linear fit:  $S_{21} = -2\beta_{nj} + c$ , with  $c \approx 0$ , are also reported.

Finally, in order to provide a further theoretical confirmation of the obtained results, a formula for the estimation of the attenuation coefficient in a realistic circular waveguide is considered. According to the approach reported in [12], for a circular waveguide of radius  $a$ , the power attenuation coefficient relative to the propagation of a  $TE_{nj}$  mode can be evaluated theoretically via the following formula:

$$\beta_{nj}^{TE} = \frac{\sqrt{\frac{\omega\mu}{2\sigma}}}{a\eta\sqrt{1-\left(\frac{f_c}{f}\right)^2}} \left[ \left(\frac{f_c}{f}\right)^2 + \frac{n^2}{\zeta_{nj}^2 - n^2} \right], \quad (14)$$

where  $\sigma$  is the metal conductivity,  $\eta = \sqrt{\mu/\epsilon}$  is the impedance of the inner medium,  $\zeta_{nj}$  is the TE mode eigenvalue,  $\omega = 2\pi f$  is the operating angular frequency, while  $f_{nj}$  is the cutoff frequency associated to the considered mode and defined by:

$$f_{nj} = \frac{\zeta_{nj}}{2\pi a\sqrt{\epsilon\mu}}. \quad (15)$$

It should be noted that, for the considered circular waveguide filled with air and surrounded by copper walls,  $\sigma = 5.7 \times 10^7$  S/m,  $\epsilon = \epsilon_0$ ,  $\mu = \mu_0$

and  $\eta$  corresponds to the vacuum impedance  $\eta_0 \approx 377 \Omega$ . The results reported in Table 1 clearly show that a very good agreement between the theoretical and numerical results has been achieved.

## 5. Conclusions

In this work, the propagation of TE superpositions carrying angular momentum in two possible guided scenarios has been investigated with the help of COMSOL Multiphysics. It is important to emphasize that the possibility to excite such modes in RF waveguides is of paramount importance not only for guided transmissions, but also

**Table 1:** Ohmic losses attenuation coefficient for a circular waveguide with radius  $a = 0.02$  m and copper walls.

$\beta_{n1}$ (dB/m)	$n = 0$	$n = 1$	$n = 2$
COMSOL (OAM)	0.0305	0.0101	0.0277
COMSOL (TE)	0.0305	0.0101	0.0277
Th. formula (14)	0.0313	0.0103	0.0284

for more general applications, since most of the antennas and the RF systems are fed via waveguides and coaxial cables. Although it is known that the above defined OAM modes do not increase the waveguide mode density and present analogous propagation properties as the standard TE modes (see Table 1), they actually represent a natural basis set for circular symmetric geometries. Therefore, it is reasonable to expect that they might bring technological simplifications in all contexts where the circular symmetry is preserved.

## 6. References

- [1] M. Tamagnone *et al.*, “Comment on ‘Reply to Comment on “Encoding many channels on the same frequency through radio vorticity: first experimental test”’”, *New Journal of Physics* **15** (2013).
- [2] E. Berglind and G. Björk, “Humblet's Decomposition of the Electromagnetic Angular Momentum in Metallic Waveguides”, *IEEE Transactions on Microwave Theory and Techniques* **62**, 779-788 (2014).
- [3] N. Bozinovic *et al.*, “Control of orbital angular momentum of light with optical fibers”, *Optics Letters* **37**, 2451-2453 (2012).
- [4] S. Ramachandran and P. Kristensen, “Optical vortices in fiber”, *Nanophotonics* **2**, 455-474 (2013).
- [5] H. Huang *et al.*, “Mode division multiplexing using an orbital angular momentum mode sorter and MIMO-DSP over a graded-index few-mode optical fibre”, *Scientific Reports* **5** (2015).
- [6] N. Bozinovic *et al.*, “Terabit-Scale Orbital Angular Momentum Mode Division Multiplexing in Fibers”, *Science* **340**, 1545-1548 (2013).
- [7] D. Zhang *et al.*, “Generating in-plane optical orbital angular momentum beams with silicon waveguides”, *IEEE Photonics Journal* **5** (2013).
- [8] W. L. Wei *et al.*, “Two monopole antennas for generating radio OAM waves in circular waveguide”, *10th European Conference on Antennas and Propagation (EuCAP 2016)*.
- [9] COMSOL Multiphysics 5.1, RF Module, <http://www.comsol.com> (2015).
- [10] J. D. Jackson, *Classical Electrodynamics*, third edition, Wiley (1999).
- [11] E. Botta and T. Bressani, *Elementi di elettromagnetismo avanzato*, Aracne (2009).
- [12] S. J. Orfanidis, *Electromagnetic Waves and Antennas*, (2014) [Online]. Available: <http://www.ece.rutgers.edu/~orfanidi/ewa>
- [13] C. A. Balanis, *Advanced Engineering Electromagnetics*, Wiley, New York (1989).